

## Chapter 5

# Approximate analytical solution of two-dimensional space-time fractional diffusion equation

### 5.1 Introduction

In this chapter, an iterative scheme is applied for the numerical solution of the space-time fractional two-dimensional reaction-advection-diffusion equation using homotopy perturbation with Laplace transform using Caputo fractional-order derivatives.

In order to analyze the diffusion of the solute in porous media in two-dimension, it is tried to develop a two-dimensional sub-diffusion physical model [30, 106] in the present chapter where the fractional differentiation is in Caputo sense.

$$\frac{\partial^\alpha u}{\partial t^\alpha} + D \frac{\partial^{\beta_1} u}{\partial x^{\beta_1}} + \frac{\partial^{\beta_2} u}{\partial y^{\beta_2}} - \gamma \frac{\partial u}{\partial x} + \frac{\partial^3 u^2}{\partial x \partial y^2} + ku(1-u) = f(x, y, t), \quad (5.1)$$

with given initial condition

$$u(x, y, 0) = u_0(x, y), \quad (5.2)$$

where  $0 < \alpha < 1, 0 \leq x \leq 1, 0 \leq y \leq 1$ ,  $\alpha$  is an arbitrary fractional order,  $k$  denotes the reaction coefficient.

Approximate analytical solutions can be computed by utilizing by linearization or series solution method. In this chapter, a new iterative Laplace transform method is studied to

find the approximate numerical solution of the considered nonlinear two-dimensional space-time fractional reaction-advection-diffusion equation. This new iterative Laplace transform method is basically a coupling of three methods viz., Laplace transform, He's polynomials and homotopy perturbation method. Integral transform methods viz., Hilbert, Fourier, Stieltjes, or Laplace transforms have a very significant role in studying the ODEs and PDEs. By use of the Laplace transform, ODEs and PDEs system have been transformed into algebraic systems. He's polynomials provides a refined series solution as shown by Ghorbani [107] and Ghorbani and Nadjafi [108]. Numerous researchers have continuously worked on the homotopy method over many years [109, 110]. Homotopy perturbation method (HPM) has been used to solve accurately, easily and effectively a wide range of nonlinear physical problems and in general, iterations converge to an exact solution rapidly after one or two iterations. A brief discussion and analysis of the HPM method are given in this chapter.

## 5.2 Basic Ideas of Laplace Transform

It is known that the Laplace transformation projects the considered time fractional reaction-diffusion equation from the time domain to the Laplacian domain. Let  $u(t)$  be the usual time-domain function of the variable  $t \geq 0$  and  $\bar{u}(s)$  is the image of  $u(t)$  under the Laplace operator in the Laplacian domain. The definition of Laplace transform can be given as

$$\bar{u}(s) = \mathcal{L}[u(t)] = \int_0^{\infty} u(t)e^{-st} dt. \quad (5.3)$$

In the above expression,  $s$  is the Laplacian parameter. The Laplace transformation for the Caputo fractional order derivative for the two-dimensional case is given as [111]

$$\mathcal{L}\left[\frac{\partial^\alpha u(x, y, t)}{\partial t^\alpha}\right] = s^\alpha \bar{u}(x, y, s) - s^{\alpha-1} u_0(x, y), \quad 0 \leq \alpha \leq 1, t \geq 0. \quad (5.4)$$

## 5.3 Homotopy Perturbation Theory and He's Polynomials

### 5.3.1 Homotopy Perturbation Method

The homotopy perturbation method (HPM) is a coupling of homotopy concept and classical perturbation technique as applied in topology. For the brief analysis of HPM for the numerical solution of nonlinear physical problems, let us assume the following nonlinear

PDE,

$$F(u) - f(x, y, t) = 0, x, y, t \in \Omega = [0, 1] \times [0, 1] \times [0, 1], \quad (5.5)$$

with the given to the boundary conditions as

$$P(u, \frac{\partial u}{\partial \eta}) = 0. \quad (5.6)$$

In the above expression,  $F$  is a generalized fractional partial differential operator,  $P$  is a boundary condition operator,  $f(x, y, t)$  is a known force term,  $\Gamma$  is the boundary region of  $\Omega$  and  $\frac{\partial u}{\partial \eta}$  denotes the derivatives along the normal direction drawn from outward directions of the  $\Omega$ .

Above mentioned fractional partial differential operator can be further divided in to two parts viz., linear part  $M(u)$  and nonlinear part  $N(u)$ , therefore equation (5.5) becomes

$$M(u) + N(u) - f(x, y, t) = 0. \quad (5.7)$$

By applying homotopy technique, we present the homotopy  $\zeta(x, y, t, \rho) \in \Omega \times [0, 1]$  with embedding parameter  $\rho \in [0, 1]$  as

$$H(\zeta, \rho) = (1 - \rho)[M(\zeta) - M(u_0)] + \rho[F(u) - f(x, y, t)] = 0. \quad (5.8)$$

The above equation can be transformed as

$$H(\zeta, \rho) = M(\zeta) - M(u_0) + \rho M(u_0) + \rho[N(\zeta) - f(x, y, t)] = 0. \quad (5.9)$$

From the equation( 5.8), it follows that

$$H(\zeta, 0) = M(\zeta) - M(u_0), \quad (5.10)$$

$$H(\zeta, 1) = F(u) - f(x, y, t). \quad (5.11)$$

Thus the process of varying  $\rho$  from zero to one is same that of  $u_0(x, y, t)$  to  $u(x, y, t)$ . This process is called deformation in topology and  $M(\zeta) - M(u_0), F(u) - f(x, y, t)$  are called homotopic. Assuming the solution of (5.8) or (5.9) in a power series of  $\rho$  and embedding parameter  $\rho$  as small quantity, we get

$$\zeta = \zeta_0 + \rho\zeta_1 + \rho^2\zeta_2 + \cdots; \quad (5.12)$$

Choosing  $\rho = 1$ , we get the approximate numerical solution of (5.5) as

$$u = \lim_{\rho \rightarrow 1} \zeta = \zeta_0 + \zeta_1 + \zeta_2 + \cdots ; \quad (5.13)$$

The coupling of the homotopy method and perturbation technique is called the homotopy perturbation method, aborting the drawbacks of ordinary perturbation technique. The author of [112] has proved the convergence of the series (5.13).

### 5.3.2 He's Polynomials

Ghorbani [107] has provided the following definitions and properties of He's polynomials.

**Definition** The He's polynomial is defined as [107]:

$$H_k(\zeta_0, \zeta_1, \zeta_2, \cdots, \zeta_k) = \frac{1}{k!} \frac{\partial^k}{\partial \rho^k} N\left(\sum_{j=0}^{\infty} \rho^j \zeta_j\right), \quad k = 0, 1, 2, \cdots ; \quad (5.14)$$

**Theorem.1** Consider  $B(\zeta)$  is a nonlinear function such that  $\zeta = \sum_{j=0}^k \rho^j \zeta_j$ , where  $\rho$  is the embedding parameter, then we have

$$\left[\frac{\partial^k}{\partial \rho^k} N(\zeta(\rho))\right]_{\rho=0} = \left[\frac{\partial^k}{\partial \rho^k} N\left(\sum_{j=0}^{\infty} \rho^j \zeta_j\right)\right]_{\rho=0} = \left[\frac{\partial^k}{\partial \rho^k} N\left(\sum_{j=0}^k \rho^j \zeta_j\right)\right]_{\rho=0}. \quad (5.15)$$

**Proof.** See [107].

## 5.4 Application On Considered Model

In this section of the chapter, the iterative Laplace scheme is applied to two-dimensional nonlinear reaction-advection-diffusion equation using HPM, and He's polynomials. Our considered model can be written in general form as

$$\frac{\partial^\alpha u(x, y, t)}{\partial t^\alpha} + M(u(x, y, t)) + N(u(x, y, t)) = f(x, y, t), \quad x, y, t \in \Omega, \quad (5.16)$$

with initial condition

$$u(x, 0) = u_0(x, y). \quad (5.17)$$

In the above equation, the fractional derivative is taken in Caputo sense,  $M$  denotes the general linear operator,  $N$  stands for general nonlinear differential operator and  $f(x, y, t)$  represents the force term.

Further, using the HPM, we get

$$u(x, y, t) = \sum_{n=0}^{\infty} \rho^n u_n(x, y, t). \quad (5.18)$$

Also, the nonlinear term occurring in method can be disintegrated in terms of He's polynomials as

$$N(u(x, y, t)) = \sum_{n=0}^{\infty} \rho^n H_n(\rho). \quad (5.19)$$

In the above equation  $H_n(\rho)$  is the He's polynomial as defined in equation (5.14).

Using equation (5.19) and operating the Laplace transform on the equation (5.16), we get

$$\mathcal{L}\left[\frac{\partial^\alpha u(x, y, t)}{\partial t^\alpha}\right] + \mathcal{L}[M(u(x, y, t))] + \mathcal{L}\left[\sum_{n=0}^{\infty} \rho^n H_n(\rho)\right] = \mathcal{L}[f(x, y, t)]. \quad (5.20)$$

In view of equation (5.4) and properties of Laplace transform, we get

$$s^\alpha \bar{u}(x, y, s) = s^{\alpha-1} u_0(x, y) + \mathcal{L}[f(x, y, t)] - \{\mathcal{L}[M(u(x, y, t))] + \mathcal{L}\left[\sum_{n=0}^{\infty} \rho^n H_n(\rho)\right]\}. \quad (5.21)$$

Using inversion of Laplace transform on equation (5.21), we get

$$u(x, y, t) = K(x, y, t) - \mathcal{L}^{-1}\left\{\frac{1}{s^\alpha} \mathcal{L}[M(u(x, y, t))] + \sum_{n=0}^{\infty} \rho^n H_n(\rho)\right\}. \quad (5.22)$$

In the above equation,  $K(x, y, t)$  is the term arises due to source term and initial condition.

Now using equation (5.14) in equation (5.22), we get

$$\sum_{n=0}^{\infty} \rho^n u_n(x, y, t) = K(x, y, t) - \rho \left( \mathcal{L}^{-1}\left\{\frac{1}{s^\alpha} \mathcal{L}\left[M\left(\sum_{n=0}^{\infty} \rho^n u_n(x, y, t)\right) + \sum_{n=0}^{\infty} \rho^n H_n(\rho)\right]\right\} \right). \quad (5.23)$$

Above equation is a combination of Laplace transform, HPM and He's polynomials. Now equating the coefficients of identical powers of  $\rho$ , we find the approximate solution of the

concerned nonlinear problem as

$$\begin{aligned}
\rho^0 : u_0(x, y, t) &= K(x, y, t), \\
\rho^1 : u_1(x, y, t) &= -\mathcal{L}^{-1}\left\{\frac{1}{s^\alpha}\mathcal{L}[M(u_0(x, y, t)) + H_0(u)]\right\}, \\
\rho^2 : u_2(x, y, t) &= -\mathcal{L}^{-1}\left\{\frac{1}{s^\alpha}\mathcal{L}[M(u_1(x, y, t)) + H_1(u)]\right\}, \\
&\cdot \\
&\cdot \\
&\cdot \\
\rho^{n+1} : u_{n+1}(x, y, t) &= -\mathcal{L}^{-1}\left\{\frac{1}{s^\alpha}\mathcal{L}[M(u_n(x, y, t)) + H_n(u)]\right\}.
\end{aligned} \tag{5.24}$$

Using the above approximation and recurrence relation, the remaining terms of  $u_n(x, y, t)$  can easily be found and the desired solution in series form can be obtained. In this way, the exact solution  $u(x, y, t)$  is approximated as

$$u(x, y, t) = \lim_{L \rightarrow \infty} \sum_{n=0}^L u_n(x, y, t). \tag{5.25}$$

The above series solution converges very fast to the exact solution after a few terms.

## 5.5 Numerical Experiments

In this section, Laplace transform homotopy method is applied to solve the fractional-order two dimensional PDEs to analyze the accuracy and applicability of the proposed scheme and compared the obtained results with the exact solutions of the given examples. All the numerical computations are carried out by using the software Mathematica 11.3.

**Example 1.** Consider time-fractional PDE as

$$\frac{\partial^\alpha u(x, y, t)}{\partial t^\alpha} + \frac{\partial^3 u(x, y, t)}{\partial x^3} + \frac{\partial^3 u(x, y, t)}{\partial y^3} = 0, \quad 0 \leq y, x \leq 1, t > 0, 0 < \alpha \leq 1, \tag{5.26}$$

with the given initial condition

$$u(x, y, 0) = u_0(x, y). \tag{5.27}$$

For the above considered fractional PDE the exact solution for  $\alpha = 1$  is given by  $u(x, y, t) = \cos(y + x + 2t)$ . Hence the initial condition is given as  $u_0(x, y) = \cos(y + x)$ .

Using Laplace transform on the above fractional PDE together with initial conditions, we have

$$\mathcal{L}\left[\frac{\partial^\alpha u(x, y, t)}{\partial t^\alpha}\right] + \mathcal{L}_t\left[\frac{\partial^3 u(x, y, t)}{\partial x^3} + \frac{\partial^3 u(x, y, t)}{\partial y^3}\right] = 0. \quad (5.28)$$

Now, using equations (5.4) and (5.27) in above equation, we get

$$s^\alpha \bar{u}(x, y, s) - s^{\alpha-1} \cos(y+x) + \mathcal{L}_t\left[\frac{\partial^3 u(x, y, t)}{\partial x^3} + \frac{\partial^3 u(x, y, t)}{\partial y^3}\right] = 0. \quad (5.29)$$

It can be converted as

$$\bar{u}(x, y, s) = \frac{\cos(y+x)}{s} - \frac{1}{s^\alpha} \mathcal{L}_t\left[\frac{\partial^3 u(x, y, t)}{\partial x^3} + \frac{\partial^3 u(x, y, t)}{\partial y^3}\right]. \quad (5.30)$$

Again, implying inverse of Laplace transformation, we get

$$u(x, y, t) = \cos(y+x) - \mathcal{L}_s^{-1}\left\{\frac{1}{s^\alpha} \mathcal{L}_t\left[\frac{\partial^3 u(x, y, t)}{\partial x^3} + \frac{\partial^3 u(x, y, t)}{\partial y^3}\right]\right\}. \quad (5.31)$$

Using HPM for above equation

$$u(x, y, t) = \sum_{n=0}^{\infty} \rho^n u_n(x, y, t). \quad (5.32)$$

Using the equation (5.32) in equation (5.31) and comparing identical power of  $\rho$ , we get

$$\begin{aligned} \rho^0 : u_0(x, y, t) &= \cos(y+x), \\ \rho^1 : u_1(x, y, t) &= -\mathcal{L}^{-1}\left\{\frac{1}{s^\alpha} \mathcal{L}[(D_x^3 + D_x^3)u_0]\right\} = \frac{-(2t^\alpha) \sin(y+x)}{\Gamma(\alpha+1)}, \\ \rho^2 : u_2(x, y, t) &= -\mathcal{L}^{-1}\left\{\frac{1}{s^\alpha} \mathcal{L}[(D_x^3 + D_x^3)u_1]\right\} = \frac{-4t^{2\alpha} \cos(y+x)}{\Gamma(2\alpha+1)}, \\ \rho^3 : u_3(x, y, t) &= -\mathcal{L}^{-1}\left\{\frac{1}{s^\alpha} \mathcal{L}[(D_x^3 + D_x^3)u_2]\right\} = \frac{8t^{3\alpha} \sin(y+x)}{\Gamma(3\alpha+1)}, \\ &\cdot \\ &\cdot \end{aligned} \quad (5.33)$$

Hence, We get the solution in series form as

$$u(x, y, t) = \cos(y+x) + \frac{-(2t^\alpha) \sin(y+x)}{\Gamma(\alpha+1)} + \frac{-4t^{2\alpha} \cos(y+x)}{\Gamma(2\alpha+1)} + \frac{8t^{3\alpha} \sin(y+x)}{\Gamma(3\alpha+1)} + \cdots; \quad (5.34)$$

The approximate series solution in (5.34) is rapidly converges to exact solution after few approximate terms.

For  $\alpha = 1$ , the above series solution can be written as

$$u(x, y, t) = \left(1 - \frac{(2t)^2}{2!} + \dots\right) \cos(y + x) - \left(2t - \frac{(2t)^3}{3!} + \dots\right) \sin(y + x). \quad (5.35)$$

The above series solution can be written in closed form as

$$u(x, y, t) = \cos(2t) \cos(y + x) - \sin(2t) \sin(y + x) = \cos(y + x + 2t). \quad (5.36)$$

Figure 5.1 demonstrates the comparison of the absolute error between the exact and numerical solutions for the above-considered example for  $\alpha = 1$  at  $t = 0.5$ . From Figure 5.1, it is clear that the numerical solution has good agreement with the given exact solution.

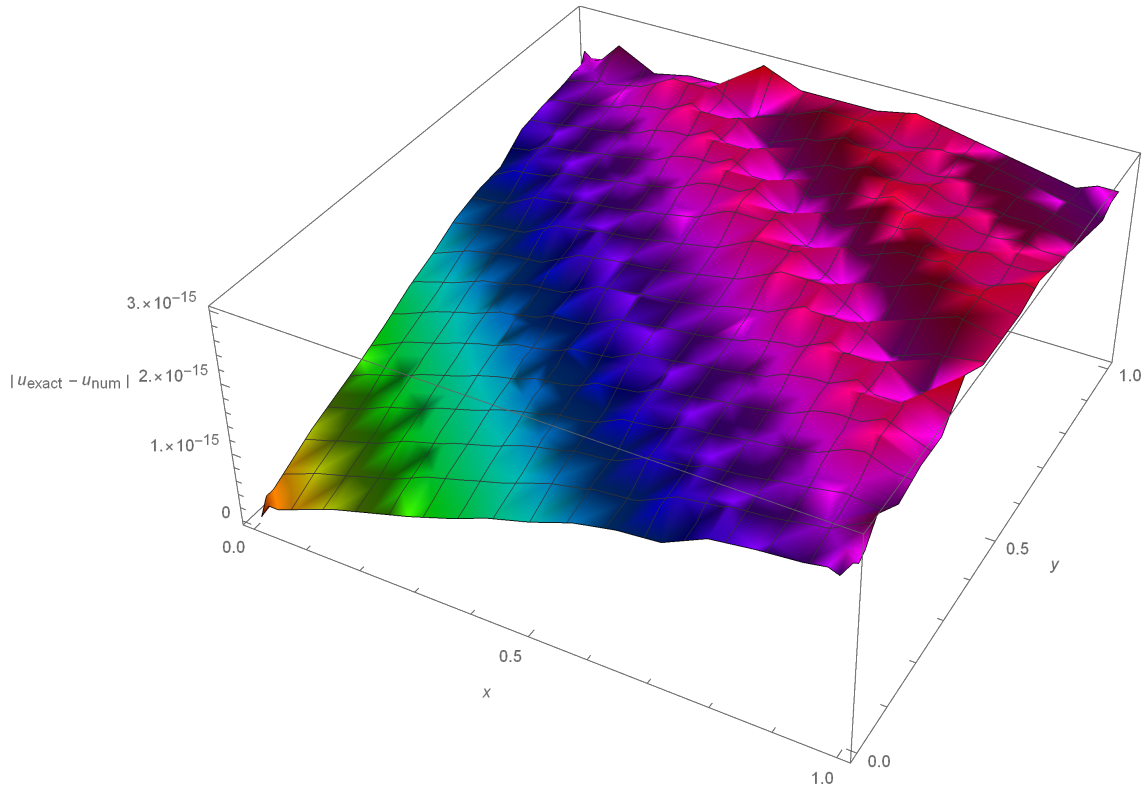


FIGURE 5.1: Plots of the absolute error between the exact and the numerical solutions vs.  $x$  and  $y$ . for  $\alpha = 1$  and  $t = 0.5$ .

Fig.5.1 shows that the approximate solution is approximately accurate to the exact solution even for few initial terms. The better convergence can be achieved with the increase in number of terms.

**Example 2.** Here we consider the nonlinear two-dimensional time fractional nonlinear Zakharov-Kuznetsov equation (ZKE) to find its approximate numerical solution by the

proposed efficient technique. It can be written as

$$D_t^\alpha u + \frac{1}{8}(u^2)_{xxx} + (u^2)_x + \frac{1}{8}(u^2)_{xyy} = 0, \quad t > 0, 0 \leq y, x \leq 1, 0 < \alpha \leq 1. \quad (5.37)$$

For the given initial condition  $u(x, y, 0) = \frac{4}{3}\varrho \sinh^2(y + x)$ , the exact solution for  $\alpha = 1$  is  $u(x, y, t) = \frac{4}{3}\varrho \sinh^2(x + y - \varrho t)$ . Following the method given in section (5.4), we have the recurrence relation for the above nonlinear equation as

$$u_{n+1}(x, y, t) = -\mathcal{L}^{-1}\left\{\frac{1}{s^\alpha} \mathcal{L}[H_n(u)]\right\}. \quad (5.38)$$

In general, He's polynomial is given by equation (5.14) and few initial terms of He's polynomials for equation (5.37) can be found as

$$\begin{aligned} H_0(u) &= \frac{1}{8}(u_0^2)_{xxx} + (u_0^2)_x + \frac{1}{8}(u_0^2)_{xyy}, \\ H_1(u) &= (2u_0u_1)_x + \frac{1}{8}(2u_0u_1)_{xxx} + \frac{1}{8}(2u_0u_1)_{xyy}, \\ H_2(u) &= (u_1^2 + 2u_0u_2)_x + \frac{1}{8}(u_1^2 + 2u_0u_2)_{xxx} + \frac{1}{8}(u_1^2 + 2u_0u_2)_{xyy}, \\ &\cdot \\ &\cdot \\ &\cdot \end{aligned} \quad (5.39)$$

Thus approximate numerical solution in the series form can be found from the equation (5.38) and is given as

$$u(x, y, t) = \lim_{Z \rightarrow \infty} \sum_{n=0}^Z u_n(x, y, t). \quad (5.40)$$

The above series solution converges to the exact solution very fast after a few terms.

The comparison of the absolute error between the exact and approximate numerical solutions for the above-considered example for  $\alpha = 1$  at  $t = 0.5$  and  $\varrho = 0.001$  is demonstrated in Figure 5.2. It is clear that the numerical solution has good agreement with the exact solution.

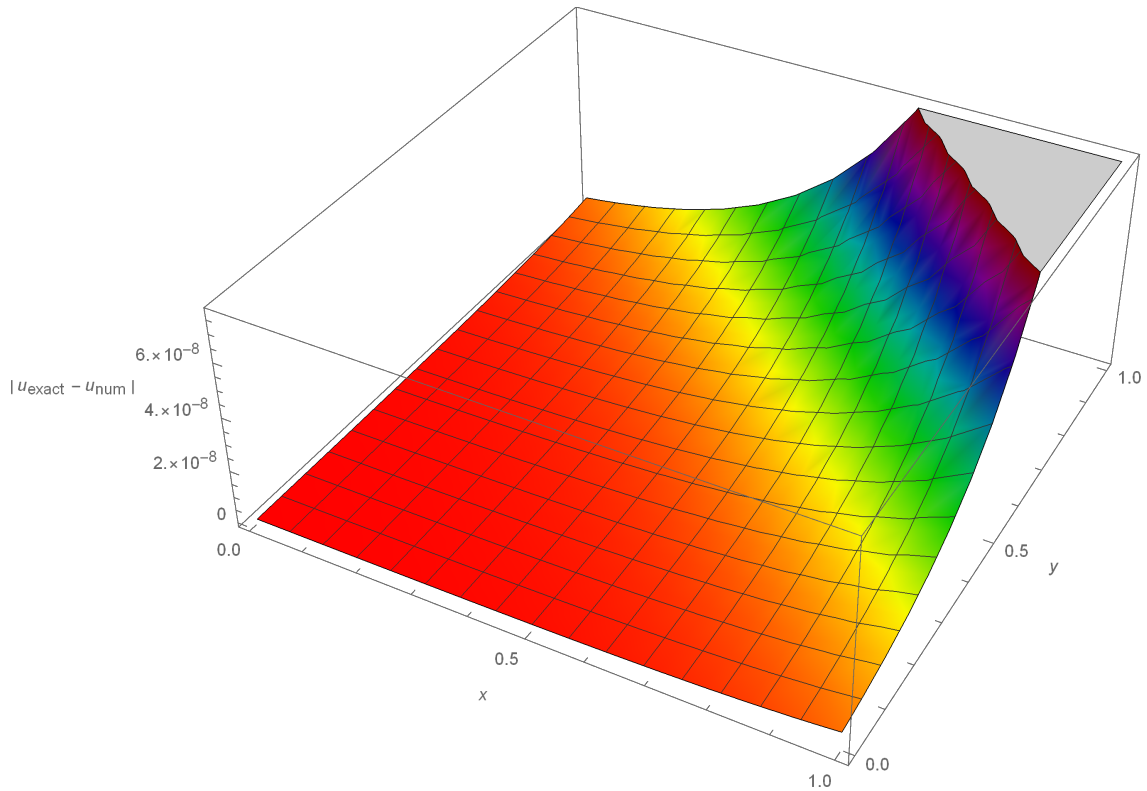


FIGURE 5.2: Plots of the absolute error between the exact and the numerical solutions vs.  $x$  and  $y$ . for  $\alpha = 1$  and  $t = 0.5$ .

Fig.5.2 shows that the obtained numerical solution is approximately accurate to the exact solution even for few initial terms. The better convergence can be achieved with increase in the number of terms. In Table 5.1, the absolute error for proposed analytical method is given and numerically compared with the error given by Senol et al.[113] for various values of  $x, y$  and  $t$  for  $\alpha = 1$ . On the observation of Table 5.1, it is concluded that our proposed method is efficient and reliable as compared to method given by Senol et al.[113]. Again the data of CPU time shows that it takes minimum time to obtain accurate result showing that the method is computationally effective to solve the two-dimensional systems.

TABLE 5.1: Comparison of absolute errors for  $\alpha = 1$ 

x	y	t	Proposed Method	Senol et al.[113]		CPU Time
			(Absolute Errors)	PIA Error	RPSM Error	(second)
0.1	0.1	0.2	$3.87777 \times 10^{-11}$	$3.85217 \times 10^{-7}$	$3.85217 \times 10^{-7}$	7.03
		0.3	$5.81646 \times 10^{-11}$	$5.75911 \times 10^{-7}$	$5.75912 \times 10^{-7}$	7.02
		0.4	$7.75502 \times 10^{-11}$	$7.65350 \times 10^{-7}$	$7.65352 \times 10^{-7}$	7.03
0.6	0.6	0.2	$4.86344 \times 10^{-9}$	$4.66337 \times 10^{-5}$	$4.66389 \times 10^{-5}$	7.06
		0.3	$7.29353 \times 10^{-9}$	$6.86056 \times 10^{-5}$	$6.86314 \times 10^{-5}$	7.06
		0.4	$9.72253 \times 10^{-9}$	$8.98243 \times 10^{-5}$	$8.99046 \times 10^{-5}$	7.08
0.9	0.9	0.2	$5.76576 \times 10^{-8}$	$5.12131 \times 10^{-4}$	$5.14241 \times 10^{-4}$	7.07
		0.3	$8.64231 \times 10^{-8}$	$7.38186 \times 10^{-4}$	$7.48450 \times 10^{-4}$	7.09
		0.4	$1.15147 \times 10^{-7}$	$9.57942 \times 10^{-4}$	$9.89139 \times 10^{-4}$	7.10

## 5.6 Numerical Results and Discussion

After being a justification of the accuracy and effectiveness of the proposed method, the author has been motivated to solve our two-dimensional nonlinear space-time fractional-order model (5.1) with the initial condition (5.2) as  $u_0(x, y) = x^2 + y$ . The variations of the solute concentration  $u(x, y, t)$  vs. the column length  $y$  and time  $t$  at  $x = 0.5$  for various values of the fractional order time parameter  $\alpha$  for conservative case ( $k = 0$ ) and non-conservative case ( $k \neq 0$ ) are calculated numerically for two dimensional fractional order reaction-advection-diffusion equation, which are displayed graphically through Figs. 5.3 - 5.7.

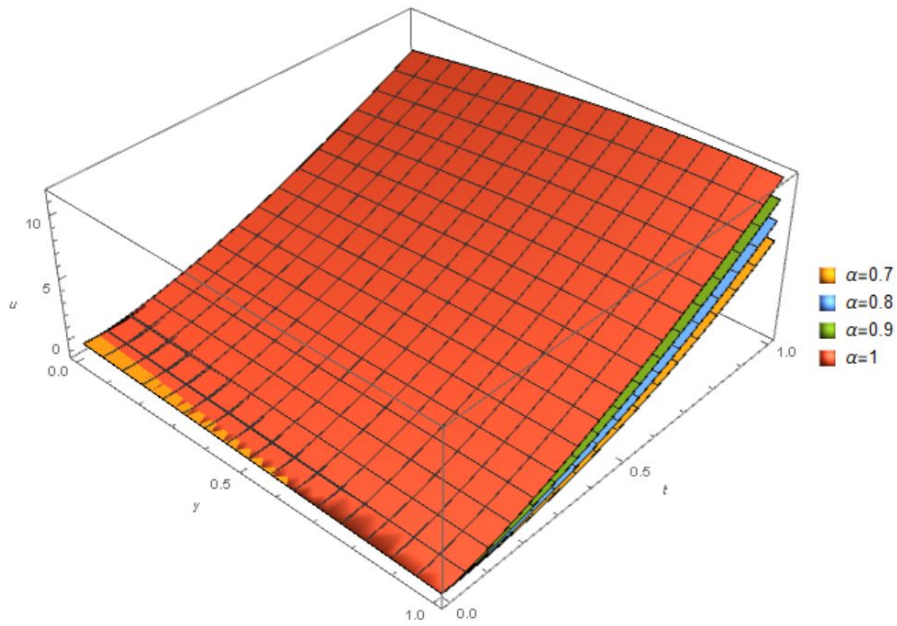


FIGURE 5.3: Plots of the field variable  $u(x, y, t)$  vs.  $y$  and  $t$  at  $x = 0.5$  for  $k = 0, \gamma = -1$  and for different values of  $\alpha$ .

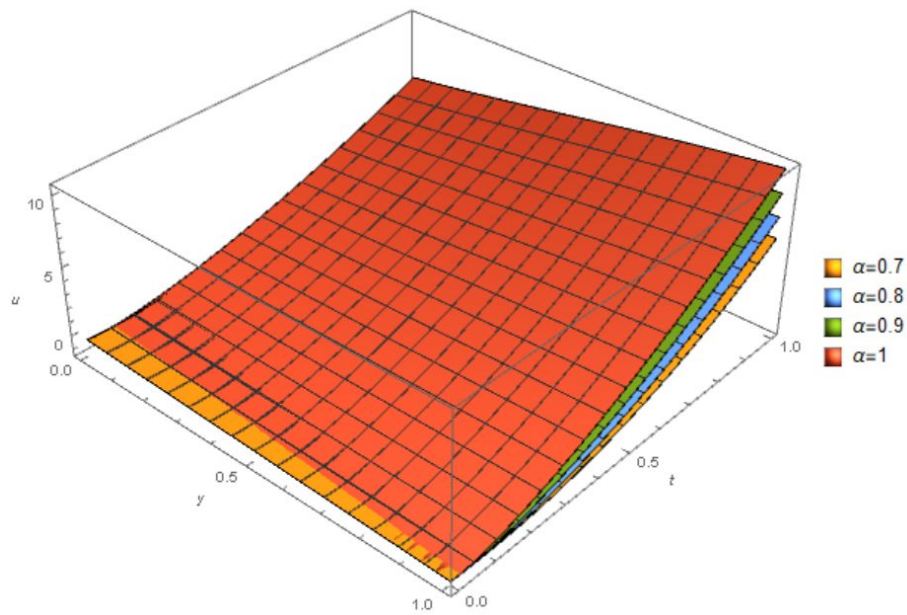


FIGURE 5.4: Plots of the field variable  $u(x, y, t)$  vs.  $y$  and  $t$  at  $x = 0.5$  for  $k = -1, \gamma = -1$  and for different values of  $\alpha$ .

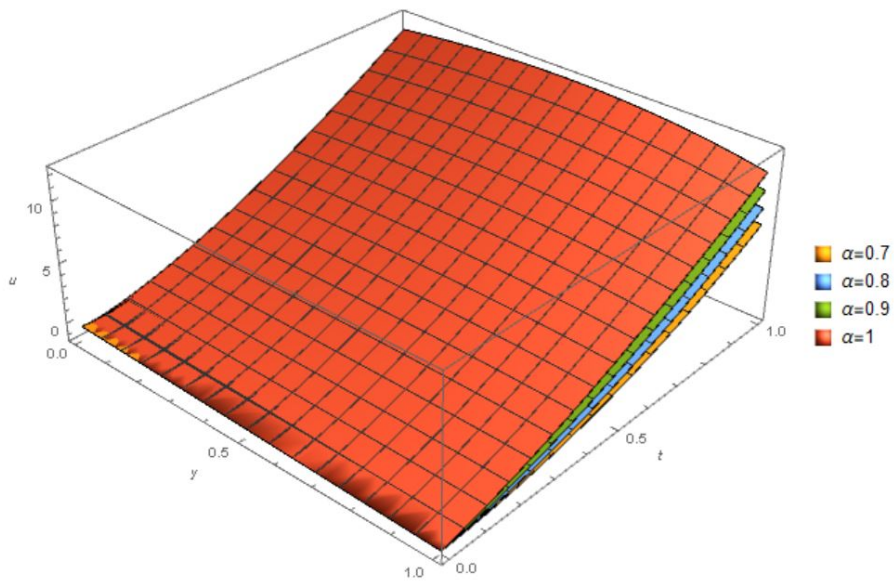


FIGURE 5.5: Plots of the field variable  $u(x, y, t)$  vs.  $y$  and  $t$  at  $x = 0.5$  for  $k = 1, \gamma = -1$  and for different values of  $\alpha$ .

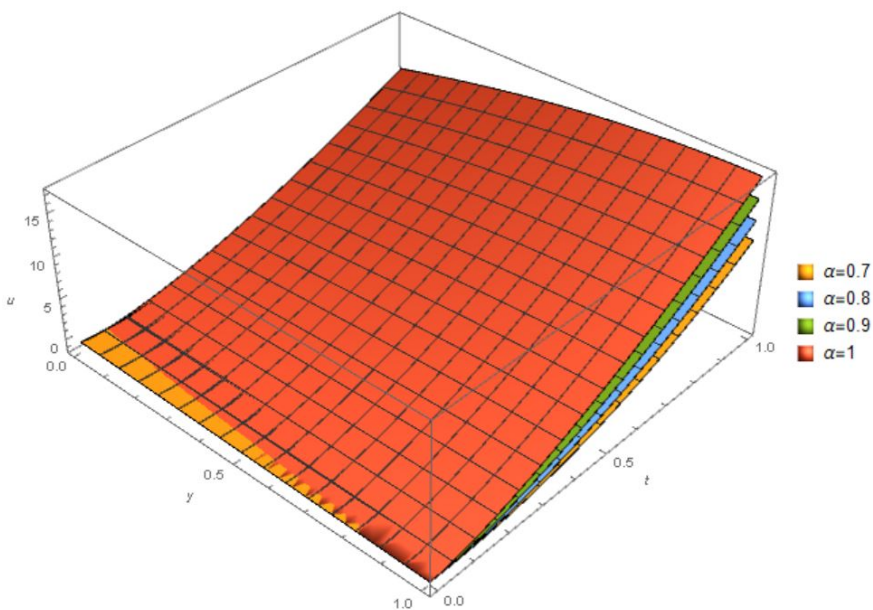


FIGURE 5.6: Plots of the field variable  $u(x, y, t)$  vs.  $y$  and  $t$  at  $x = 0.5$  for  $k = 1, \gamma = 1$  and for different values of  $\alpha$ .

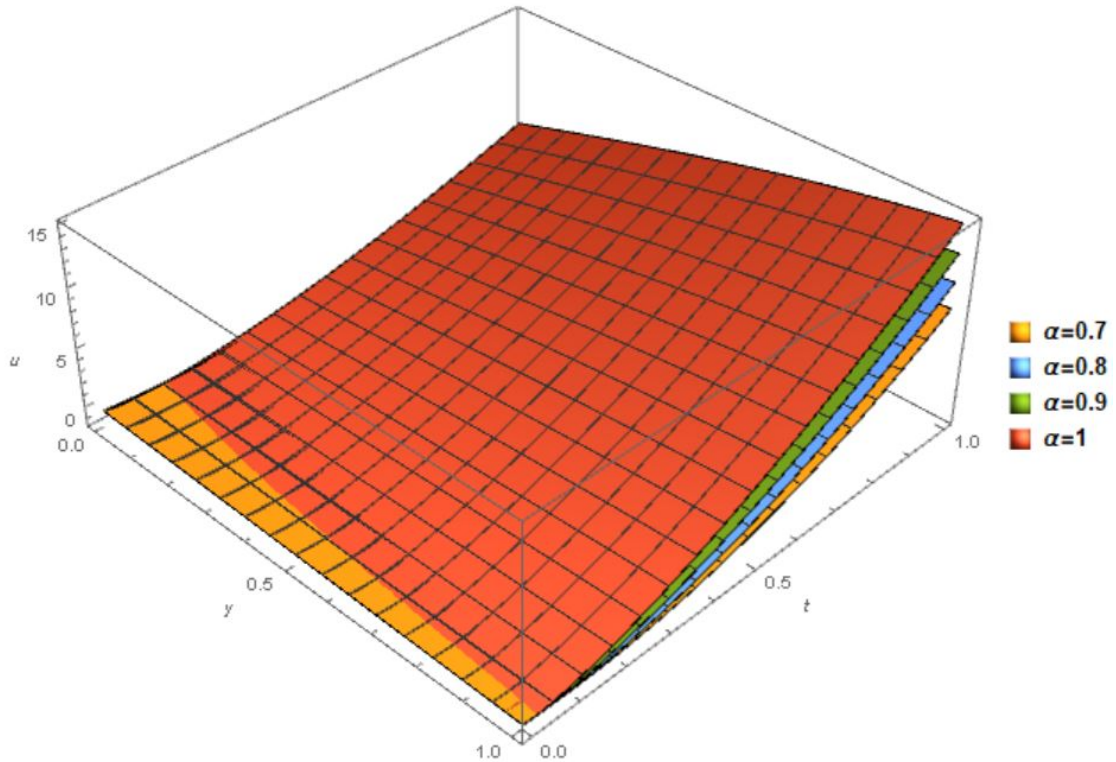


FIGURE 5.7: Plots of the field variable  $u(x, y, t)$  vs.  $y$  and  $t$  at  $x = 0.5$  for  $k = 0, \gamma = 1$  and for different values of  $\alpha$ .

The effect of reaction term on the solution profile for various values of the fractional-order time derivative is found by comparing the numerical results shown in Figs. 5.3 - 5.5 for  $k = 0, -1$  and  $k = 1$ , respectively for advection term  $\gamma = -1$ . Fig. 5.6 and Fig. 5.7 are for  $k = 1$  and  $k = 0$ , respectively for advection term  $\gamma = 1$ . It is seen that the overshoots of sub-diffusion are increased as the system advances towards fractional-order from standard order. It is also seen from the figures that dampings are found due to the presence of sink term ( $k = -1$ ). Fig.5.6 and Fig.5.7 reveal the distribution of probability density function  $u(x, y, t)$  at  $x = 0.5$  for the various cases of  $\alpha$  due to  $k = 0$  and also due to presence of source term  $k = 1$ , which clearly show that physical importance of the presence of source term for the enhancement of stability region.

## 5.7 Conclusion

In the present scientific work, the homotopy perturbation Laplace transform method has been considered for finding the approximate analytical solution of the recognized

two-dimensional reaction-advection-diffusion problem with fractional derivative in Caputo sense. An efficient technique has been provided to find the approximate numerical solution in a series form which converges rapidly after a few terms. The results obtained in solving the considered two-dimensional problem plays a notable role in analyzing the behavior of many physical problems in porous media. The present chapter has achieved three significant consequences. First one is the demonstration of the damping nature of the probability density function  $u(x, y, t)$  of the considered two-dimensional reaction-advection-diffusion equation of fractional order as well as integer order by the use of the proposed technique. The second one is the pictorial representations of the nature of overshoots of solute concentration due to the presence of the reaction term. The last one is the solute concentration when the considered system approaches fractional-order to integer-order in the presence of source and sink terms.